

Supplementary Information for

Epithelial to Mesenchymal Plasticity and Differential Response to Therapies in Pancreatic Ductal Adenocarcinoma

Rebecca L. Porter^{a,d}, Neelima KC Magnus^a, Vishal Thapar^a, Robert Morris^a, Annamaria Szabolcs^a, Azfar Neyaz^a, Anupriya S. Kulkarni^a, Eric Tai^a, Abhijit Chougule^{a,c}, Alessandra Hillis^a, Gabriel Golczer^a, Hongshan Guo^a, Teppei Yamada^{a,b}, Tomohiro Kurokawa^{a,b}, Chittampalli Yashaswini^a, Matteo Ligorio^{a,b}, Kevin D. Vo^a, Linda Nieman^a, Andrew S. Liss^b, Vikram Deshpande^{a,c}, Michael S. Lawrence^{a,c,f}, Shyamala Maheswaran^{a,b}, Carlos Fernandez-Del Castillo^b, Theodore S. Hong^{a,e}, David P. Ryan^{a,d}, Peter J. O'Dwyer^h, Jeffrey A. Drebinⁱ, Cristina R. Ferrone^{b,2}, Daniel A. Haber^{a,d,g,1,2}, David T. Ting^{a,d,1,2}

Massachusetts General Hospital ^aCancer Center, Departments of ^bSurgery, ^cPathology, ^dMedicine, ^eRadiation Oncology, and Harvard Medical School, Boston, MA 02114, USA.

^fBroad Institute of Harvard and MIT, Cambridge, MA 02142, USA.

^gHoward Hughes Medical Institute, Chevy Chase, Maryland 20815, USA.

^hAbramson Cancer Center, University of Pennsylvania, Philadelphia, PA 19014, USA.

ⁱDepartment of Surgery, Memorial Sloan Kettering Cancer Center, New York, NY, 10065, USA.

¹ Address correspondence to
Daniel A. Haber (dhaber@mgh.harvard.edu)
Massachusetts General Hospital Cancer Center
Building 149, 13th, Rm 207
Charlestown, Massachusetts 02129

and

David T. Ting (dting1@mgh.harvard.edu)
Massachusetts General Hospital Cancer Center
Building 149, 13th Street, Rm 6-618B
Charlestown, Massachusetts 02129

² These authors contributed equally to this work

This PDF file includes:

Figures S1 to S4

Figure S1

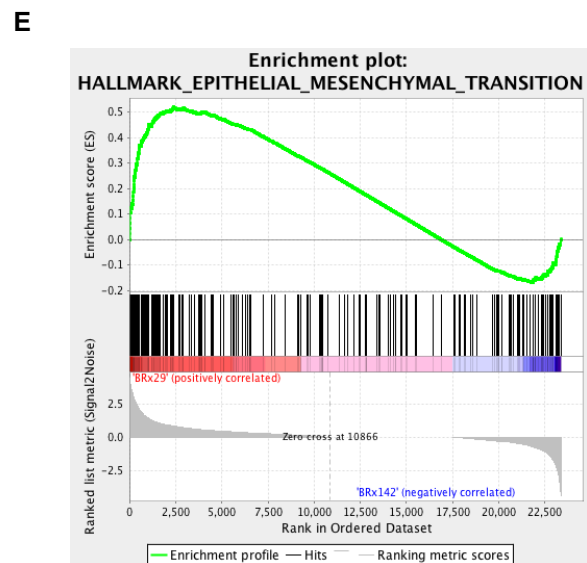
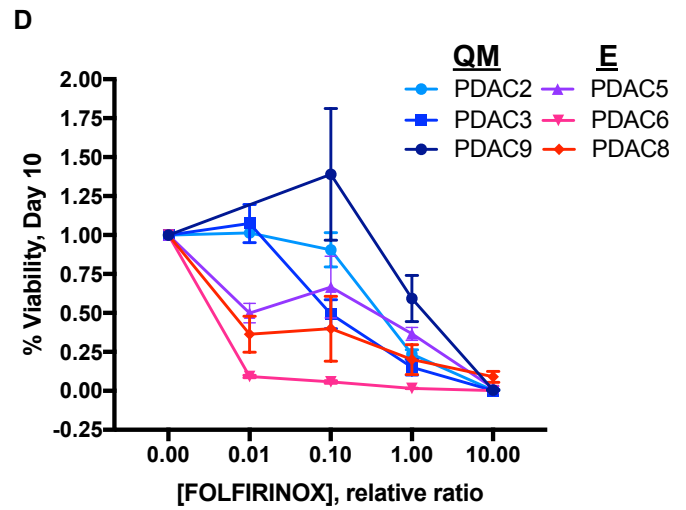
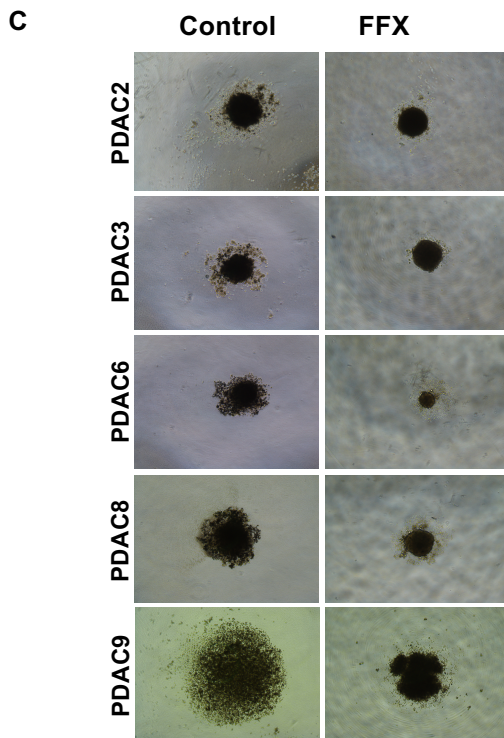
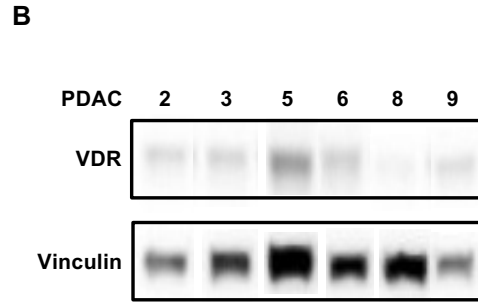
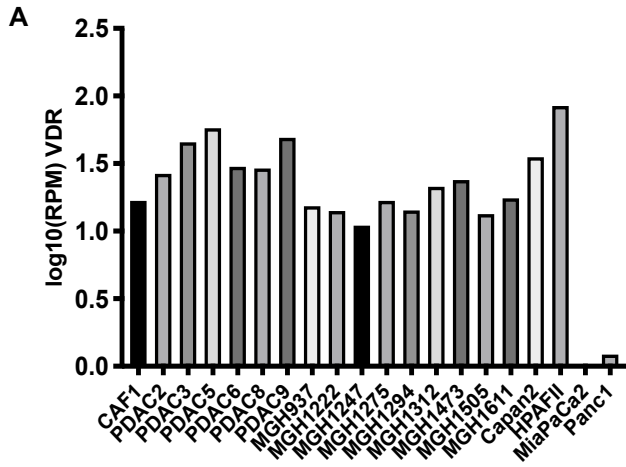


Figure S1:

(A) Expression of VDR across a panel of patient-derived PDAC cell lines and commercially available cell lines Capan2, HPAFII, MiaPaCa2 and Panc1, as determined by RNA-seq. (B) VDR protein levels in PDAC cell lines, as determined by Western Blot. (C) Representative 4x images of PDAC tumorspheres grown in 96 well ultra low attachment plates captured at Day 7 following FFX or vehicle-control dosing. (D) Dose response curve of PDAC cell lines to FFX in vitro. (E) Enrichment plot for Hallmark EMT pathway in FFX-treated PDAC cell lines.

Figure S2

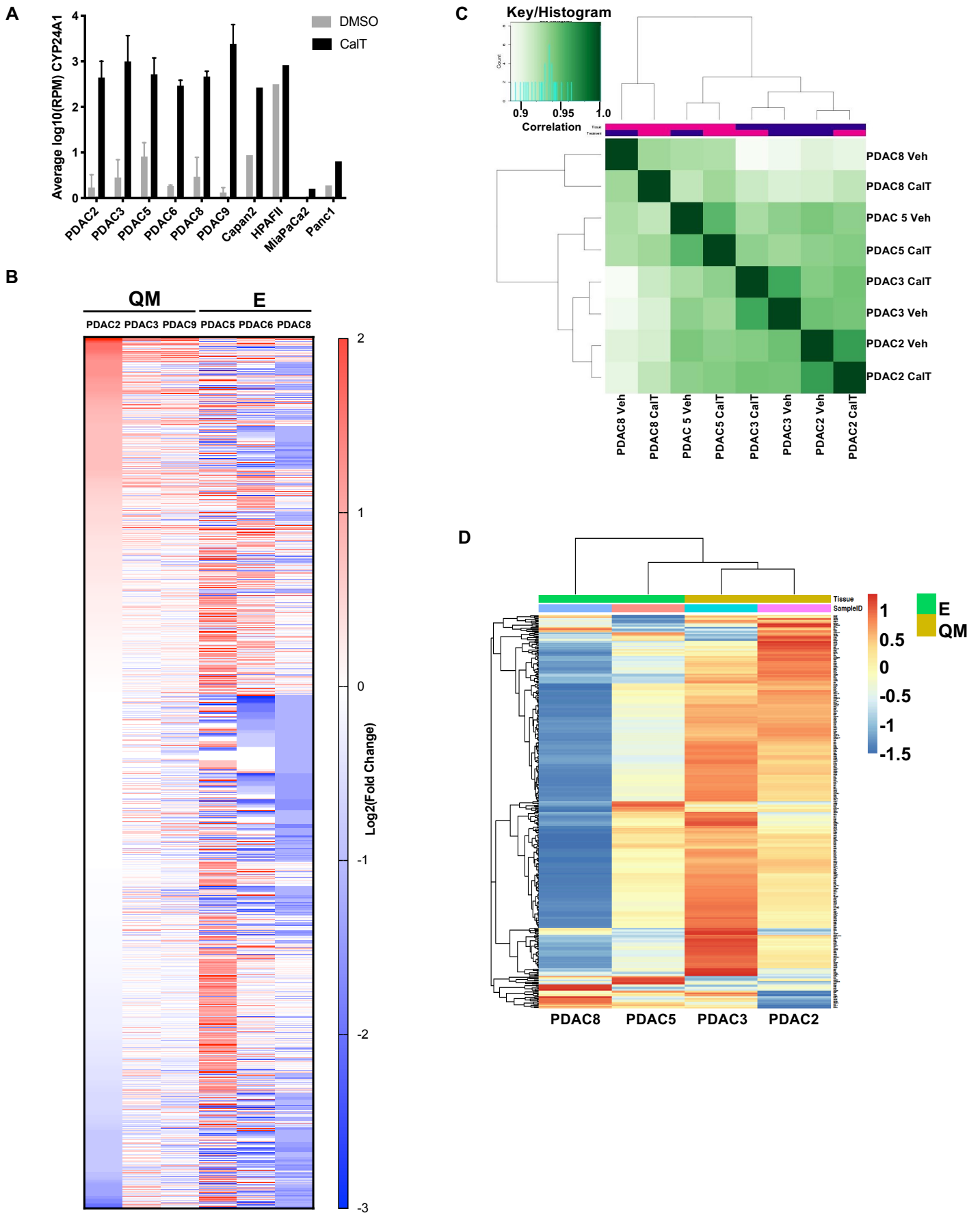


Figure S2:

(A) CYP24A1 expression in patient-derived PDAC cell line and commercially available PDAC cell line spheroids following 5 days of CalT treatment compared with vehicle control as determined by RNA-seq, expressed as log₁₀ reads per million (RPM). Error bars indicate s.d. (B) Expression heat map of genes whose expression is 2-fold up- or down-regulated with CalT treatment in any single PDAC cell line. Scale bar represents log₂(fold change) relative expression in CalT-treated samples compared with vehicle control. (C) Correlation heat map of CalT-treated and vehicle-control PDAC ATAC-seq samples using chromatin accessibility peaks across the genome. (D) Heatmap of Z score row-normalized log₂fold changes of ATACseq openness, clustering promoter region peaks containing VDRE motif on each sample.

Figure S3

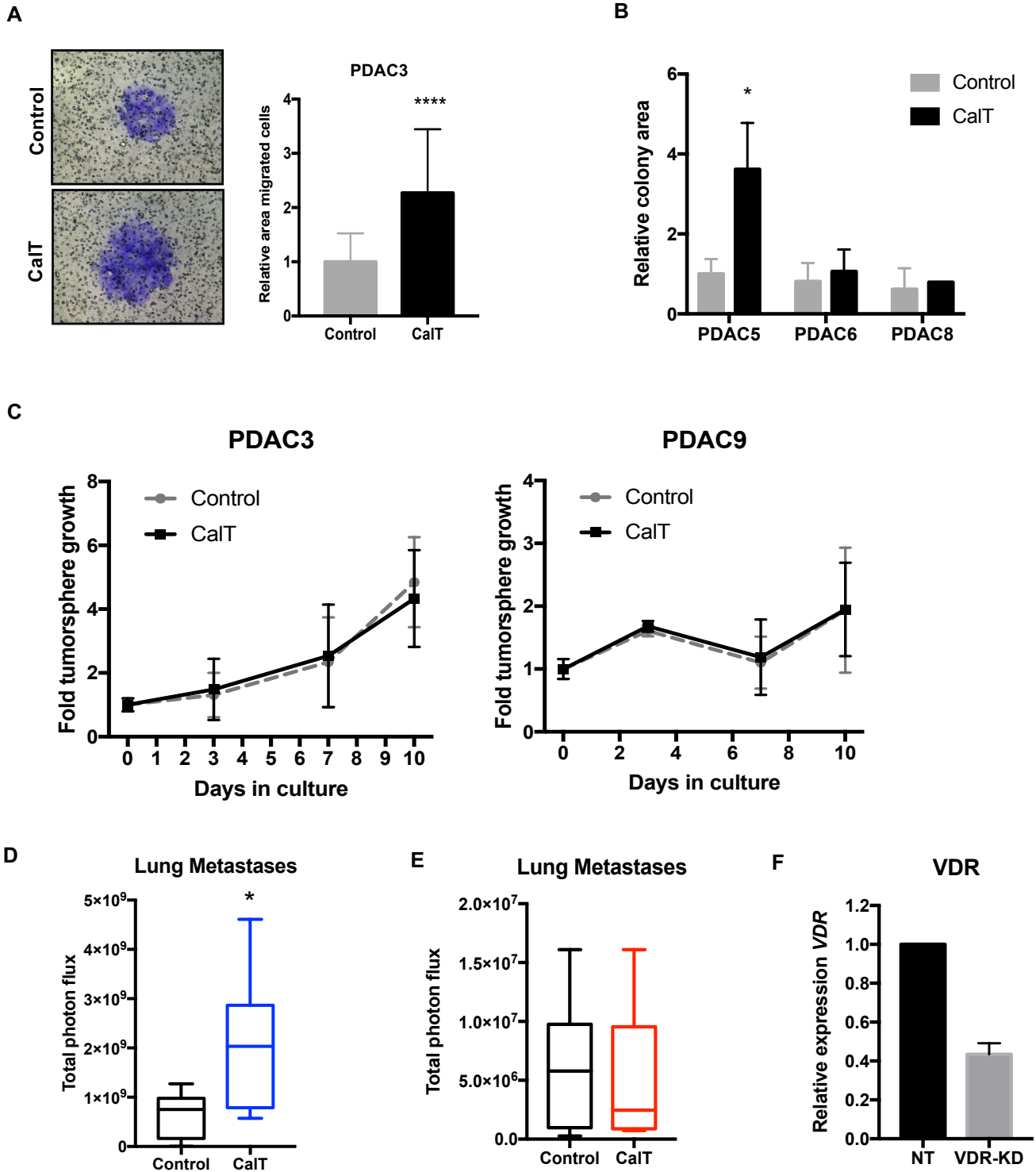


Figure S3:

(A) Representative images showing migration of QM PDAC cells from an intact spheroid 24hr after seeding on 8mm filters in the presence or absence of CaIT. Quantification of area covered by stained cells in three independent experiments (n=3-8 per experiment) is shown. (B) Quantification of total colony area in four independent experiments using E PDAC cell lines (n=3 per experiment). (C) Relative tumorsphere growth over time in 3D culture in the presence or absence of 10nM CaIT as determined by CellTiterGlo viability assay and expressed as fold tumorsphere growth over Day 0 control. Graphs summarize three independent experiments per cell lines and error bars represent standard deviation. (D) Quantitation of metastases in explanted lungs on day of sacrifice from mice receiving control or CaIT-treated PDAC9 cells. *p<0.05. (E) Quantitation of metastases in explanted lungs on day of sacrifice from mice receiving control or CaIT-treated PDAC6 cells. (F) Relative expression of VDR in PDAC9 cells transduced with VDR shRNA (VDR-KD) compared with non-target shRNA control (NT).

Figure S4

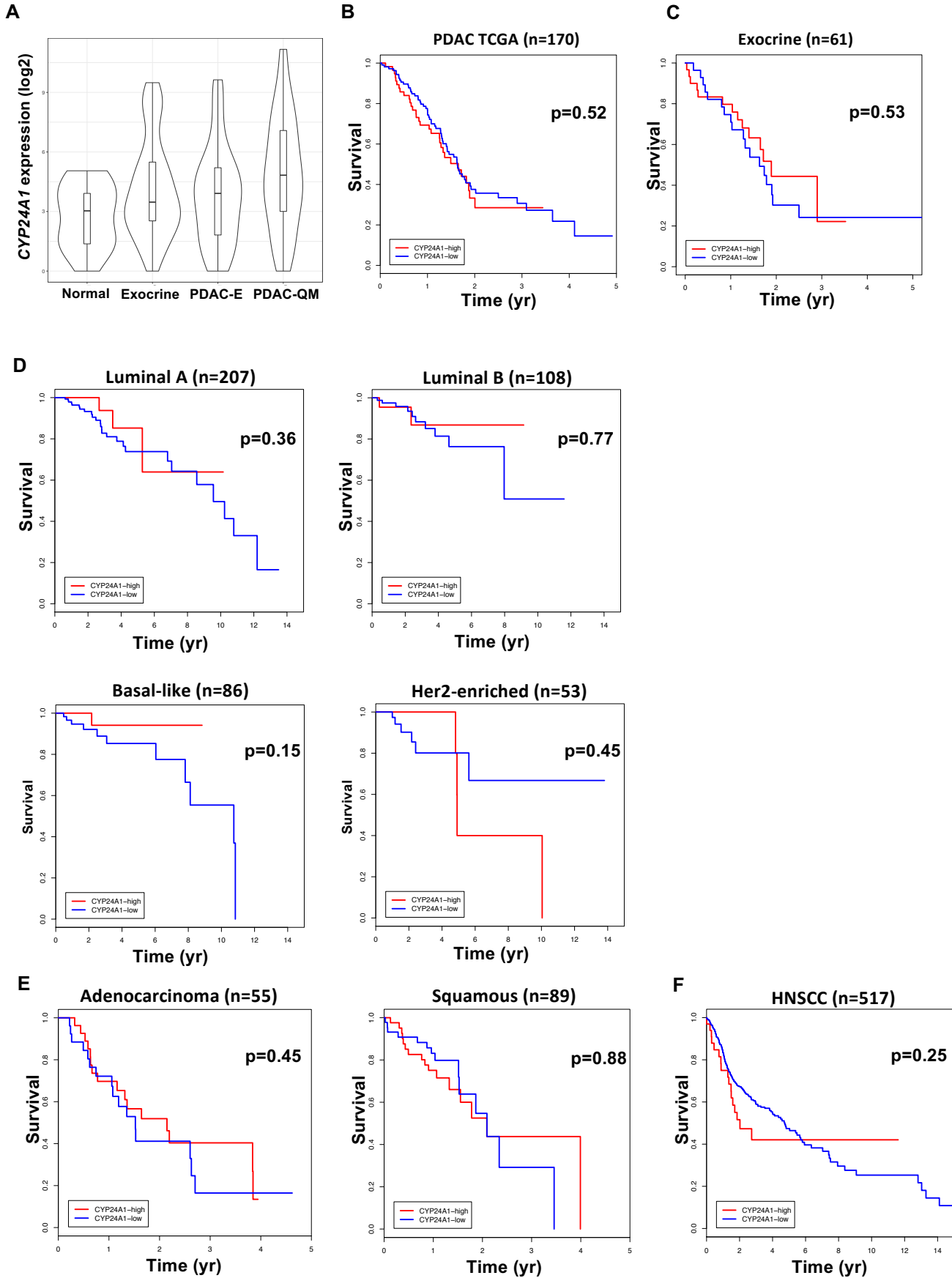


Figure S4:

(A) Violin plots depicting *CYP24A1* expression levels, expressed as log₂(RPM), across normal tissues, exocrine pancreas tumors, E subtype and QM subtype PDAC tumors from the TCGA. (B) Kaplan-Meier survival curves for high vs. low *CYP24A1* expression in all PDAC tumors (E, QM, exocrine-like) in the TCGA dataset. (C) Kaplan-Meier survival curves for high vs. low *CYP24A1* expression in exocrine-like tumors from the TCGA dataset. (D-F) Kaplan-Meier survival curves for high vs. low *CYP24A1* expression in subsets of breast cancer tumors (D), esophageal cancer (E) and head and neck squamous cell carcinoma (F) as labeled.